# The role of intermixing in all-optical switching of synthetic-ferrimagnetic multilayers

Cite as: AIP Advances **9**, 125133 (2019); https://doi.org/10.1063/1.5129892
Submitted: 02 October 2019 . Accepted: 05 November 2019 . Published Online: 23 December 2019

M. Beens, M. L. M. Lalieu, R. A. Duine, and B. Koopmans

# The role of intermixing in all-optical switching of synthetic-ferrimagnetic multilayers

Cite as: AIP Advances 9, 125133 (2019); doi: 10.1063/1.5129892
Presented: 6 November 2019 • Submitted: 2 October 2019 •
Accepted: 5 November 2019 • Published Online: 23 December 2019



M. Beens,[1,a)] M. L. M. Lalieu,[1] R. A. Duine,[1,2] and B. Koopmans[1]

## AFFILIATIONS

[1] Department of Applied Physics, Eindhoven University of Technology, P.O. Box 513, 5600 MB Eindhoven, The Netherlands
[2] Institute for Theoretical Physics, Utrecht University, Leuvenlaan 4, 3584 CE Utrecht, The Netherlands

**Note:** This paper was presented at the 64th Annual Conference on Magnetism and Magnetic Materials.
[a)] **Corresponding author:** m.beens@tue.nl

## ABSTRACT

We present a theoretical study of single-pulse all-optical switching (AOS) in synthetic-ferrimagnetic multilayers. Specifically, we investigate the role of interface intermixing in switching Co/Gd bilayers. We model the laser-induced magnetization dynamics in Co/Gd bilayers using the microscopic three-temperature model for layered magnetic systems. Exchange scattering is included, which mediates angular momentum transfer between the magnetic sublattices. In this work, each layer is represented by one atomic monolayer of a GdCo alloy with an arbitrary Co concentration, allowing Co/Gd bilayers with an intermixed interface to be modelled. Our results indicate that within the model intermixing of the Co/Gd interface reduces the threshold fluence for AOS significantly. We show that intermixing does not qualitatively affect the switching mechanism and leads to an increase of the propagation speed of the switching front.



All-optical switching (AOS) refers to switching magnetization by femtosecond laser pulses and was first observed in ferrimagnetic GdFeCo alloys.[1–3] Single-pulse AOS has gained extensive attention due to the intriguing underlying physics and its potential for ultrafast data writing technologies. Recently, it was demonstrated that not only alloys, but also Pt/Co/Gd stacks can be switched by the use of a single linearly polarized laser pulse.[4] This synthetic-ferrimagnetic multilayer has proven to be an ideal candidate for the integration of AOS in future magnetic memory devices.[5] Moreover, it has been shown that AOS in Pt/FM/Gd is very robust and can be achieved for a relatively large ferromagnetic (FM) layer thickness, i.e., the switching mechanism in synthetic-ferrimagnetic multilayers is independent of magnetization compensation.[6]

The key ingredient of single-pulse AOS is that the material system contains multiple magnetic sublattices, coupled by an antiferromagnetic exchange interaction. The exchange coupling drives the magnetization reversal by transferring angular momentum between the sublattices.[7] This insight was corroborated by simulations using the atomistic Landau-Lifshitz-Gilbert equation.[8–12] An alternative approach was derived by extending the microscopic three-temperature model (M3TM) to multisublattice magnets.[13] The latter includes exchange scattering as the mechanism for angular momentum transfer between the sublattices. Very recently, we extended this model to describe single-pulse AOS in Co/Gd bilayers.[6] Based on the simulations, it was concluded that the robustness of AOS in Pt/FM/Gd is caused by the non-local character of the switching mechanism. For example, the mechanism in Co/Gd bilayers can be understood as a front of reversed Co magnetization that, after laser-pulse excitation, nucleates at the Co/Gd interface and propagates through the Co layer driven by exchange scattering. An important question is to what extent the properties of the Co/Gd interface, e.g., the amount of intermixing, affect the switching mechanism within the model.

In this work, we show that intermixing reduces the threshold fluence for AOS in Co/Gd bilayers and leads to faster propagation of the switching front. We perform simulations of AOS in Co/Gd bilayers including an intermixed interface. In order to do this, we define each atomic monolayer in the Co/Gd bilayer as a GdCo alloy with an arbitrary Co concentration. By choosing the appropriate Co concentration for each monolayer, a Co/Gd bilayer including an intermixed (alloyed) interface is modelled. We use the M3TM including exchange scattering to describe the magnetization dynamics of the

system.[6,13] We present phase diagrams that show the reduced threshold fluence. Finally, we analyse the role of intermixing on the propagating switching mechanism by calculating the switching times for the individual atomic monolayers.

To describe the system of interest, we introduce multiple spin subsystems that are all coupled to a single electron and phonon system.[13] We consider the same approximations as the basic M3TM,[14] where the electrons are described as a spinless free electron gas and the phonons are treated within the Debye model. The electron and phonon system are internally thermalized and the electron temperature $T_e$ and phonon temperature $T_p$ are homogeneous. The spin specific heat is neglected. The electron system contains an energy source term which represents the laser pulse. Heat diffusion to the substrate is included in the phonon system as an energy dissipation term. The spin subsystems are treated within a Weiss mean field approach and all compose a magnetic sublattice with at each lattice site $D_s = \mu_{at}/2S$ spins, where $\mu_{at}$ is the atomic magnetic moment (in units of the Bohr magneton $\mu_B$) and $S$ is the spin quantum number.

We consider a system of $N$ atomic monolayers. Each layer $i$ corresponds to a two-dimensional $Gd_{1-x_i}Co_{x_i}$ alloy with Co concentration $x_i$. Hence, all the layers consist of two magnetic sublattices, one for each compound. We define $m_{Co,i}$ and $m_{Gd,i}$ as the normalized magnetization of a specific magnetic sublattice in layer $i$ ($i \in [1, N]$). In the following, we only take into account nearest neighbour interactions. First, we introduce the bulk exchange splitting for a $Gd_{1-x_i}Co_{x_i}$ alloy with Co concentration $x_i$[6]

$$\Delta^{\text{bulk}}_{\text{Co},i} = x_i \gamma_{\text{Co-Co}} m_{\text{Co},i} + (1 - x_i)\gamma_{\text{Co-Gd}} m_{\text{Gd},i}, \quad (1)$$

$$\Delta^{\text{bulk}}_{\text{Gd},i} = x_i \gamma_{\text{Gd-Co}} m_{\text{Co}} + (1 - x_i)\gamma_{\text{Gd-Gd}} m_{\text{Gd},i}, \quad (2)$$

where we defined $\gamma_{kl} = j_{kl} z D_{s,l} S_l$ ($k, l \in \{\text{Co, Gd}\}$) in terms of the (intra- or intersublattice) exchange coupling constant $j_{kl}$ and the number of nearest neighbours $z$.

To express the exchange splitting in the $N$ layers of $Gd_{1-x_i}Co_{x_i}$, we assume that the separate layers lie in the (111) plane of an fcc lattice. In that case, each atom has 6 nearest neighbours in the same layer and 3 nearest neighbours in each adjacent layer. The exchange splitting for a specific compound in layer $i$ is

$$\Delta_{\text{Co},i} = \frac{1}{4}\Delta^{\text{bulk}}_{\text{Co},i-1} + \frac{1}{2}\Delta^{\text{bulk}}_{\text{Co},i} + \frac{1}{4}\Delta^{\text{bulk}}_{\text{Co},i+1}, \quad (3)$$

$$\Delta_{\text{Gd},i} = \frac{1}{4}\Delta^{\text{bulk}}_{\text{Gd},i-1} + \frac{1}{2}\Delta^{\text{bulk}}_{\text{Gd},i} + \frac{1}{4}\Delta^{\text{bulk}}_{\text{Gd},i+1}. \quad (4)$$

Note that for a homogeneous system (i.e., $x_i = x$ for all $i$) the exchange splitting reduces to the bulk value, equation (1) and (2). For simplicity, we describe both the Co and Gd by a $S = 1/2$ system. Hence, all the spin subsystems correspond to a two-level system, splitted by the energy $\Delta_{\text{Co},i}$ or $\Delta_{\text{Gd},i}$. We note that the model can be easily extended to $S = 7/2$ for Gd.[6]

In our model, the dynamics of the magnetic sublattices is driven by two interactions. First, Elliott-Yafet spin-flip scattering results in angular momentum transfer between the magnetic sublattices and the phonon system. The basic M3TM is used to describe the resulting magnetization dynamics.[14] Secondly, we include exchange scattering, which corresponds to electron-electron scattering with an opposing spin flip. Exchange scattering mediates angular momentum transfer between the different magnetic sublattices. The resulting magnetization dynamics is derived from Fermi's golden rule, using the exact same procedure as reported in Ref. 6.

The result is a system of coupled differential equations, which expresses $dm_{k,i}/dt$ for all compounds $k$ and layers $i$. Each equation will contain terms for the angular momentum transfer (by exchange scattering) between (i) the two different compounds in the same layer, (ii) two different compounds in adjacent layers and (iii) the same compound in adjacent layers. These terms will implicitly depend on the Co concentration of each layer via the coordination number, i.e., the number of nearest neighbours of a specific compound and layer. The latter involves the same counting procedure as the derivation of the exchange splitting in equation (3) and (4). Furthermore, all the exchange scattering terms depend on the corresponding matrix element of the exchange scattering Hamiltonian and the probability of an electron-electron scattering event to occur. For the mathematical description of these terms and a detailed discussion about the system parameters, we refer to Ref. 6.

The normalized magnetization $m_{k,i}(t)$ is calculated by solving the system of coupled differential equations numerically. In these simulations, the temporal profile of the laser pulse is given by $P(t) = (P_0/(\pi\sqrt{\sigma}))\text{Exp}(-(t - t_0)^2/\sigma^2)$, where $P_0$ is the laser pulse energy density and $\sigma$ is the pulse duration, which is set to 50 fs. Furthermore, the ambient temperature $T_{\text{amb}}$ is set to 295 K.

We construct three phase diagrams that display the occurrence of AOS in Co/Gd bilayers as a function of the laser pulse energy $P_0$ and the number of Co monolayers $N_{\text{Co}}$. Figure 1(a) shows the phase diagram for an ideal Co/Gd bilayer, without intermixing of the Co/Gd interface. Figure 1(b) displays the phase diagram for an intermixed Co/Gd interface, described by replacing the two layers adjacent to the interface by a $Gd_{0.5}Co_{0.5}$ alloy. In Fig. 1(c) the intermixing region is further extended to four layers of $Gd_{0.5}Co_{0.5}$. Note that the definition of $N_{\text{Co}}$ is unchanged (see insets Fig. 1(a)–(c)). The color scheme indicates whether the average magnetization of the Co layers is reversed after relaxation, which is determined by calculating its sign at $t = 100$ ps. Figure 1(d)–(e) show the dynamics of the normalized magnetization for an ideal Co/Gd bilayer, and are presented to clarify the color scheme of the phase diagrams. The blue regions indicate that AOS has occurred successfully, i.e., the magnetization is reversed (Fig. 1(d)). The white regions indicate that AOS has not occurred and the magnetization remained in its initial direction (Fig. 1(e)). The grey regions correspond to the situation where the phonon temperature $T_p$ has exceeded the Curie temperature $T_C$. In the experiments this would likely result in the creation of a multidomain state.[15]

Figure 1(a) clearly shows, as was reported earlier,[6] that the Co/Gd bilayers can be switched for a relatively large number of Co layers $N_{\text{Co}}$, i.e., for a large Co layer thickness. Moreover, the threshold fluence increases as a function of $N_{\text{Co}}$. The qualitative behaviour observed in the phase diagram can be understood by the switching mechanism in the Co/Gd bilayers. First, the Co layers near the interface are switched, creating a front of reversed Co magnetization. Subsequently, the front propagates through the system driven by exchange scattering between adjacent layers.[6] This propagating mechanism will continue until all Co layers are switched.

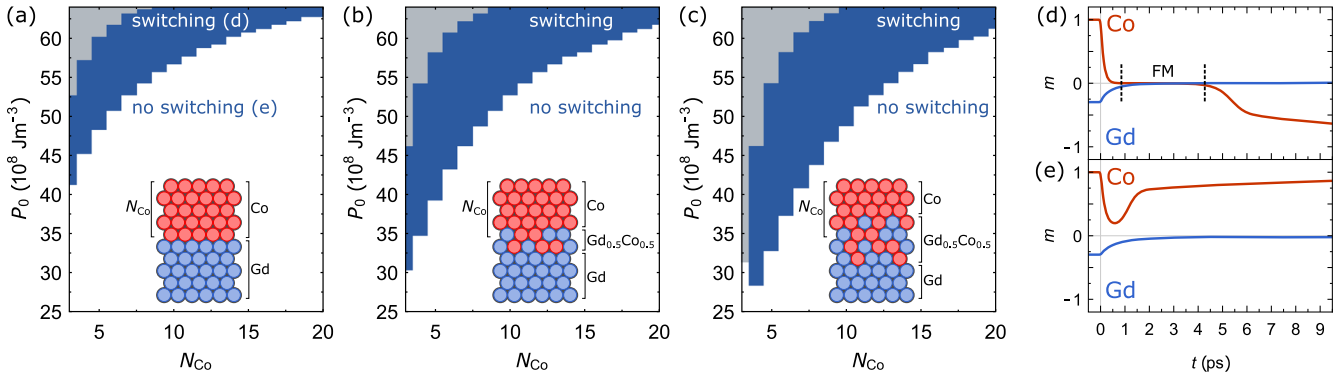


**FIG. 1**. Phase diagrams for AOS as a function of the laser pulse energy $P_0$ and the number of Co monolayers $N_{Co}$ in a Co/Gd bilayer. Figure (a) shows the phase diagram for an ideal Co/Gd bilayer, without intermixing at the Co/Gd interface (see inset Fig. (a)). Figure (b) shows the phase diagram for Co/Gd bilayers including intermixing, modelled by replacing the two layers adjacent to the interface by two layers of $Gd_{0.5}Co_{0.5}$ (see inset Fig. (b)). Figure (c) shows a similar phase diagram, but now the intermixing region is extended to four layers (see inset Fig. (c)). The blue regions indicate a switch in the final state and the white regions indicates no switch. Grey indicates that the phonon temperature $T_p$ exceeds the Curie temperature $T_C$. The insets in (a)-(c) schematically show the modelled system. Figure (d) and (e) show the normalized magnetization of the Co an Gd layer as a function of time, in case of switching (d) and no switching (e).

The phase diagram for the Co/Gd bilayers including intermixing shows the same qualitative behaviour, as is depicted in Fig. 1(b). Interestingly, for relatively thin Co layers ($N_{Co}$ = 3-5), the threshold fluence is reduced by ~25% compared to the system without intermixing. The reduction of the threshold fluence can be understood by (i) in case of intermixing there is effectively more angular momentum transfer between Co and Gd sublattices and (ii) a decrease of the Curie temperature $T_C$. Note that the observed value for the threshold fluence is now comparable to the value found in the simulations for the alloys.[6]

Figure 1(c) shows that increasing the size of the intermixing region leads to a further reduction of the threshold fluence. However, no switching is observed for $N_{Co}$ = 3. This can be understood from the fact that this particular system is very similar to a homogeneous $Gd_{0.5}Co_{0.5}$ alloy, which can not be switched because the total magnetic moment is not close to compensation.[6]

Following the analysis of the phase diagrams, the question that arises is to what extent the intermixing of the Co/Gd interface influences the properties of the propagating switching mechanism. Figure 2(a) shows a detailed analysis of the switching mechanism in a system of 10 Co and 5 Gd layers. It displays the time at which each individual Co layer is reversed as a function of the layer index. The Co layers are labeled from 1 to 10, where the index 1 represents the Co layer adjacent to the Co/Gd interface. We consider the same three systems as in the phase diagrams (with $N_{Co}$ = 10), which are schematically presented in Fig. 2(b)–(d). Note that the layer indices are unchanged despite the addition of an intermixing region. In Fig. 2(a), the red dots represent an ideal Co/Gd bilayer, without intermixing (see Fig. 2(b)). The blue and yellow dots represent a Co/Gd bilayer with an intermixing region of two and four layers respectively (see Fig. 2(c)–(d)). Figure 2(a) shows that in all three systems the layers are switched consecutively starting with the layers near the interface, which defines the propagating switching mechanism. However, in case of an ideal Co/Gd interface, the layer adjacent to the interface acts differently. This is, in the approximation of only nearest-neighbour interactions, caused by the exchange field resulting from the slowly demagnetizing Gd layer.[6] This field slows down the demagnetization and reversal process of the inner Co layer due to the antiferromagnetic exchange coupling between Co and Gd. In the presence of intermixing, this effect is shifted to the unlabelled layers. Importantly, the blue and yellow dots clearly show that the propagating characteristics of the switching mechanism are maintained after including intermixing within the model.

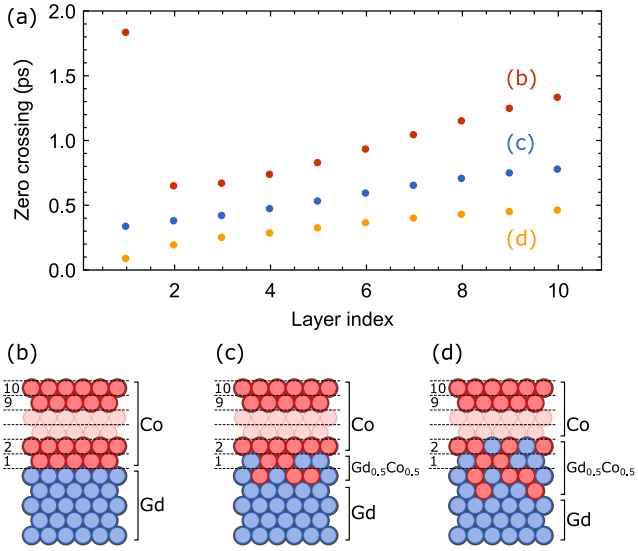


**FIG. 2**. (a) The time at which each atomic Co monolayer is reversed for the systems indicated in Figure (b)-(d) and $P_0 = 60 \cdot 10^8 \mathrm{Jm}^{-3}$. Figure (b) displays a system of 10 Co and 5 Gd atomic monolayers. The Co layers are numbered 1-10, where index 1 refers to the layer adjacent to the interface. Figure (c) and (d) show the systems including intermixing, with the Co/Gd interface replaced by two (c) and four (d) layers of $Gd_{0.5}Co_{0.5}$.

To analyse the propagation speed of the switching front, we focus on the region from layer 3 to layer 10, which consists entirely of Co in all three systems (Fig. 2(b)–(d)). The propagation speed can be approximated from the interval between the switching times of layer 3 and 10 and the corresponding distance the switching front has travelled. Here, we take 0.2 nm for the thickness of one atomic monolayer of Co.[4] For the system without intermixing, the propagation speed is then given by approximately 2.1 km/s. For the systems including intermixing, we find a propagation speed of 3.9 km/s (Fig. 2(c)) and 6.6 km/s (Fig. 2(d)) respectively. Hence, intermixing of the Co/Gd interface increases the propagation speed of the switching front significantly. As noted before, intermixing leads to effectively more angular momentum transfer between the Co and Gd sublattices near the interface, increasing the magnetization gradient in the Co layer. This leads to a larger propagation speed of the switching front, because the speed is related to the magnitude of the magnetization gradient.

To conclude, within the model we considered in this paper, intermixing leads to a significant reduction of the threshold fluence for AOS compared to the ideal Co/Gd interface. Furthermore, intermixing does not affect the qualitative properties of the switching mechanism in Co/Gd bilayers. Quantitatively, intermixing increases the speed of propagation. Hence, previously reported statements about the switching mechanism in ideal Co/Gd bilayers can be generalized to bilayers including an intermixed Co/Gd interface.

This work was part of the research programme of the Foundation for Fundamental Research on Matter (FOM), which is part of the Netherlands Organisation for Scientific Research (NWO).

## REFERENCES

[1] C. D. Stanciu, F. Hansteen, A. V. Kimel, A. Kirilyuk, A. Tsukamoto, A. Itoh, and Th. Rasing, "All-optical magnetic recording with circularly polarized light," Phys. Rev. Lett. **99**, 047601 (2007).

[2] I. Radu, K. Vahaplar, C. Stamm, T. Kachel, N. Pontius, H. A. Dürr, T. A. Ostler, J. Barker, R. F. L. Evans, R. W. Chantrell, A. Tsukamoto, A. Itoh, A. Kirilyuk, Th. Rasing, and A. V. Kimel, "Transient ferromagnetic-like state mediating ultrafast reversal of antiferromagnetically coupled spins," Nature **472**, 205 (2011).

[3] T. A. Ostler, J. Barker, R. F. L. Evans, R. W. Chantrell, U. Atxitia, O. Chubykalo-Fesenko, S. El Moussaoui, L. Le Guyader, E. Mengotti, L. J. Heyderman, F. Nolting, A. Tsukamoto, A. Itoh, D. Afanasiev, B. A. Ivanov, A. M. Kalashnikova, K. Vahaplar, J. Mentink, A. Kirilyuk, Th. Rasing, and A. V. Kimel, "Ultrafast heating as a sufficient stimulus for magnetization reversal in a ferrimagnet," Nat. Commun. **3**, 666 (2012).

[4] M. L. M. Lalieu, M. J. G. Peeters, S. R. R. Haenen, R. Lavrijsen, and B. Koopmans, "Deterministic all-optical switching of synthetic ferrimagnets using single femtosecond laser pulses," Phys. Rev. B **96**(R), 220411 (2017).

[5] M. L. M. Lalieu, R. Lavrijsen, and B. Koopmans, "Integrating all-optical switching with spintronics," Nat. Commun. **10**, 110 (2019).

[6] M. Beens, M. L. M. Lalieu, A. J. M. Deensn, R. A. Duine, and B. Koopmans, "Comparing all-optical switching in synthetic-ferrimagnetic multilayers and alloys" (2019), arXiv:1908.07292.

[7] J. H. Mentink, J. Hellsvik, D. V. Afanasiev, B. A. Ivanov, A. Kirilyuk, A. V. Kimel, O. Eriksson, M. I. Katsnelson, and Th. Rasing, "Ultrafast spin dynamics in multisublattice magnets," Phys. Rev. Lett. **108**, 057202 (2012).

[8] T. A. Ostler, R. F. L. Evans, R. W. Chantrell, U. Atxitia, O. Chubykalo-Fesenko, I. Radu, R. Abrudan, F. Radu, A. Tsukamoto, A. Itoh, A. Kirilyuk, Th. Rasing, and A. V. Kimel, "Crystallographically amorphous ferrimagnetic alloys: Comparing a localized atomistic spin model with experiments," Phys. Rev. B **84**, 024407 (2011).

[9] U. Atxitia, P. Nieves, and O. Chubykalo-Fesenko, "Landau-Lifshitz-Bloch equation for ferrimagnetic materials," Phys. Rev. B **86**, 104414 (2012).

[10] J. Barker, U. Atxitia, T. A. Ostler, O. Hovorka, O. Chubykalo-Fesenko, and R. W. Chantrell, "Two-magnon bound state causes ultrafast thermally induced magnetisation switching," Scientific Reports **3**, 3262 (2013).

[11] S. Gerlach, L. Oroszlany, D. Hinzke, S. Sievering, S. Wienholdt, L. Szunyogh, and U. Nowak, "Modeling ultrafast all-optical switching in synthetic ferrimagnets," Phys. Rev. B **95**, 224435 (2017).

[12] U. Atxitia and T. A. Ostler, "Ultrafast double magnetization switching in GdFeCo with two picosecond-delayed femtosecond pump pulses," Appl. Phys. Lett. **113**, 062402 (2018).

[13] A. J. Schellekens and B. Koopmans, "Microscopic model for ultrafast magnetization dynamics of multisublattice magnets," Phys. Rev. B **87**, 020407(R) (2013).

[14] B. Koopmans, G. Malinowski, F. Dalla Longa, D. Steiauf, M. Fähnle, T. Roth, M. Cinchetti, and M. Aeschlimann, "Explaining the paradoxical diversity of ultrafast laser-induced demagnetization," Nat. Mater. **9**, 259–265 (2010).

[15] J. Gorchon, R. B. Wilson, Y. Yang, A. Pattabi, J. Y. Chen, L. He, J. P. Wang, M. Li, and J. Bokor, "Role of electron and phonon temperatures in the helicity-independent all-optical switching of GdFeCo," Phys. Rev. B **94**, 184406 (2016).